Impurity Behavior in ITER and Helical Burning Plasmas with Internal Transport Barriers

Kozo YAMAZAKI, Ikuhiro YAMADA, Tetsutarou OISHI, Hideki ARIMOTO and Tatsuo SHOJI

Nagoya University, Chikusa-ku, Nagoya 464-8603 Japan

(Received: 2 September 2008 / Accepted: 10 December 2008)

The impurity transport simulation code TOTAL (TOroidal Transport Analysis Linkage) consisting of 1-D(dimensional) transport and 2- or 3-D equilibrium is developed for analyzing tokamak and helical burning plasmas controlled by feedback scheme with gas puffing, pellet fueling injection and heating power modulations. In this code multi-species of impurity ions can be treated including neoclassical transport and adding radial electric field effects in helical plasmas. The permissible impurity concentrations for ITER operations are clarified first, and impurity radial profiles, especially carbon, iron and tungsten density profiles, are evaluated in tokamak and helical reactors. The effect of internal transport barrier (ITB) on impurity dynamics is also analyzed for ITER-like plasmas, and impurity shielding or concentrating mechanism induced by edge density modification is clarified.

Keywords: impurity transport, tungsten, neoclassical transport, internal transport barrier, ITER, tokamak reactor, helical reactor

1. Introduction

In order to access to the ignition regime of the fusion reactor, impurity effects are crucial for sustaining long burn of tokamak and helical plasmas. The density limit might be related to the impurity radiation power loss in both tokamak and helical systems. Moreover, in order to check the access to ignition regime it is important to clarify the plasma radial profile and the local energy balance including impurity effects in burning plasmas with internal transport barrier (ITB).

In order to clarify these issues, reactor plasma analysis is performed using the TOTAL (toroidal transport analysis linkage) code as reported in Ref. [1]. The impurity analysis using TOTAL code has already been done for tokamak plasmas [2] and helical plasmas [3]. In this paper, we include multi-species impurity (especially carbon, iron and tungsten) dynamics with ignited plasma operation with ITB formation in tokamak reactors and self-consistent ambipolar electric field in helical systems.

2. Simulation Models Including Impurity Dynamics

For studying transport of plasma and impurity ions (carbon, ion, beryllium, tungsten, others) in fusion reactors such as ITER, tokamak power plants and helical reactors, we used 1-D (dimensional) transport and 2- or 3-D equilibrium TOTAL simulation code [1-3]. The plasma equilibria with arbitrary 2-D or 3-D shapes are calculated by APOLLO [4] or VMEC [5] code for tokamak and helical systems, respectively (Table I). The plasma transport with ITB in tokamaks is calculated by rather simple semi-empirical transport model [2], the GLF23 transport model [6] and Bohm/GyroBohm mixed model with ExB flow shear against ITG mode [7] in addition to neoclassical NCLASS model [8]. In the helical plasma analysis, radial ambipolar electric filed is determined by the neoclassical transport flux including impurity flux. For the impurity charge-state dynamics, the rate equation and diffusion equation are solved using IMPDYN code [9] with ADPAC code [10].

Table I. List of Simulation Codes Linked to Toroidal Transport Linkage (TOTAL) Code

	TOTAL code[1-3]	
	<Tokamak>	<Helical>
Main	TOTAL-T	TOTAL-H
Vacuum Field	----	HSD
Equilibrium	APOLLO[4]	VMEC[5]
Neoclassical	NCLASS[8]	GIOTA
Anomalous	GLF23[6] etc.	empirical
Impurity	IMPDYN[9] + ADPAC[10]	
Synchrotron	CYTRAN[11]	

author's e-mail: yamazaki@ees.nagoya-u.ac.jp

2-1. TOTAL Plasma Simulation Code

For studying transport of fuel and impurity ions in fusion reactors, we used 1.5-D (1-D transport/2-D equilibrium for tokamak), or 2.0-D (1-D transport/3-D equilibrium for helical system) time-dependent simulation model [1] with low-Z gas and high-Z metal impurity dynamics. The plasma density n_e, n_i and temperature T_e, T_i are described by

$$\frac{\partial n_e}{\partial t}+\frac{1}{V'}\frac{\partial}{\partial \rho}V\Gamma_e = S_p, \quad \sum_i z_i n_i \approx n_e, \tag{1}$$

$$\frac{3}{2}\frac{\partial n_e T_e}{\partial t}+\frac{1}{V'}\frac{\partial}{\partial \rho}\left\{V'\left(q_e+\frac{5}{2}\Gamma_e T_e\right)\right\} = P_{He}-P_{ei}-P_{rad}-\Gamma_e E_r, \tag{2}$$

$$\frac{3}{2}\frac{\partial n_i T_i}{\partial t}+\frac{1}{V'}\frac{\partial}{\partial \rho}\left\{V'\left(q_i+\frac{5}{2}\Gamma_i T_i\right)\right\} = P_{Hi}+P_{ei}-P_{cx}+z_i\Gamma_i E_r, \tag{3}$$

using the normalized radius ρ and the volume V defined by the equilibrium magnetic surface. The radiation loss P_{rad} is the summation of bremsstrahlung, impurity line radiation and synchrotron radiation. The synchrotron radiation loss power is calculated by Trubnikov's model or non-local CYTRAN synchrotron radiation model [11], however, this synchrotron energy loss is small in the present reactor analysis assuming with good wall reflection coefficients greater than 99%.

2-2. ITB Simulation Models

In order to simulate advanced operations of tokamak and helical plasmas with internal transport barrier (ITB) and edge transport barrier (EBT), we can use several models in TOTAL code such as GLF23 model, current diffusive ballooning mode, Bhom/GyroBhom mixed model with ExB shear flow effect and so on. Here, we used mainly Bohm/GyroBohm mixed model relevant to ion temperature gradient mode wih ExB shear flow stabilization. The analyses have already been carried out without impurity and focusing on high-field-side pellet injection effects to make easy access to ITB regime [12].

2-3. Impurity Simulation Models

For the impurity dynamics, the rate equation and the diffusion equation are solved using IMPDYN code [6] coupled with ADPAK atomic physics package [7],

$$\frac{\partial n_k}{\partial t} = -\frac{1}{V'}\frac{\partial}{\partial \rho}(V\Gamma_k)+[\gamma_{k-1}n_{k-1}+\alpha_{k+1}n_{k+1}-(\gamma_k+\alpha_k)n_k]n_e+S_k, \tag{4}$$

$$\Gamma_k = \Gamma_k^{NCs}+\Gamma_k^{NCa}-D_k(\rho)\frac{\partial n_k}{\partial \rho}+V_k(\rho)n_k, \tag{5}$$

with ionization rate γ_k, recombination rate α_k and particle source term S_k. Here, diffusion constant D_k and simply modeled velocity $V_k = V(a)\bullet(r/a)$ are used for anomalous transport. The main fuel neutrals are calculated by the AURORA Monte Carlo code [13].

The neoclassical impurity flux in tokamak is expressed by

$$\Gamma_k^{NCs} = -D_k^{NC}\nabla n_k + D_k^{NC}n_k[\sum_{l\neq k}(g_{nl\to k}\nabla n_l/n_l) + g_{Ti}\nabla T_i/T_i + g_{Te}\nabla T_e/T_e]. \tag{6}$$

Within the present neoclassical theory, radial electric field effects are not included in tokamaks, different from the following helical plasmas. The neoclassical ripple transport coefficient in helical system is given by the density gradient, temperature gradient and the radial electric field [14, 15]:

$$D_k^{NCa} \propto D_{rip\nabla n}\nabla n/n + D_{rip\nabla T}\nabla T/T - ZE_r/T \tag{7}$$

Here, we adopted the neoclassical formula of fuel ions to include the impurity ions in addition to the tokamak-like axi-symmetric neoclassical flux [16].

The radial electric filed in helical system is determined by the neoclassical transport flux including impurity ions as follows,

$$\left(\sum_k z_k\Gamma_k^{NCa}(E_r)-\Gamma_e^{NCa}(E_r)\right)=0. \tag{8}$$

Here, the subscript k denotes fuel ions (D &T), helium and impurity ions. The neutral impurity density is given by

$$v_0\frac{\partial n_k}{\partial \rho} = S_0 n_e n_0. \tag{9}$$

Here, v_0 is neutral impurity velocity, and S_0 and n_e is ionization coefficient and electron density at plasma boundary.

3. Models of Tokamak and Helical Plasmas

We considered typical three burning plasmas; ITER, tokamak reactor TR-1[1] and helical reactor HR-1[1], as shown in Table II. Tokamak reactor TR-1 and helical reactor HR-1 with 1 GW electric power output obtained by the system code are evaluated comparing with ITER-like plasmas.

Table II. Typical Machine and Plasma Parameters for Three Reactors.

	ITER	TR-1	HR-1
R_p(m)	6.2	5.3	13
A_p(m)	2	1.2	-
$<a_p>$(m)	2.7	1.7	2.2
κ	1.7	2	-
δ	0.3	0.5	-
B(T)	5.3	7.1	4.6
Ip(MA)	9~15	10	-
β_N	1.8~2.6	4	-
<β>	~2	5	5
P_{fusion}(GW)	~0.5	2.7	2.3
$P_{electric}$(GW)	-	1.0	1.0

4. Impurity Simulation Results

4-1. Permissible impurity level for reactor ignition access

In order to check permissible impurity level for reactor ignition access, 10% line radiation level of the DT fusion power in the reactor have been evaluated, namely, at 50% of alpha particle heating power. Less than several % oxygen impurity is permissible, but the level of tungsten impurity should be less than several 10^{-3}%. In ITER, the critical level of impurity is, 4.0% for carbon, 0.1% for ion, and 0.008% for tungsten impurity with respect to electron density.

4-2. Impurity behavior

(1) ITER and Tokamak Reactors TR-1 plasmas

Figure1 shows the time-evolution of ITER-like plasma operation when tungsten impurity ions are accidentally flowing into plasma at 200s and the tungsten density becomes 4% of electron density. The impurity line radiation is rapidly increased at this time, and the plasma temperature is decreased.

The typical radial profile of tungsten impurity in TR-1 ignited tokamak reactor plasma with temperature internal transport barrier (ITB) at ρ~0.5 is shown in Fig.2. The large temperature gradient in ITB can assist the impurity shielding effects. However, as shown in this figure, highly-stripped charge-state tungsten impurities penetrate into the core due to high electron temperature.

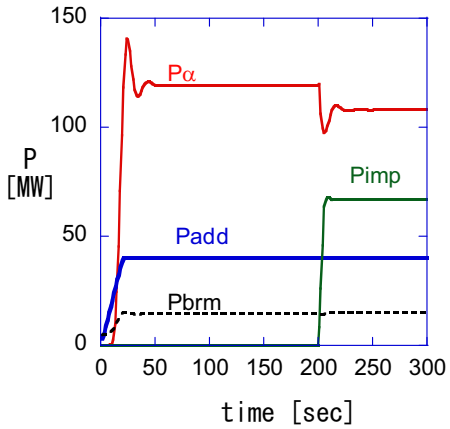

Fig.1 Effects of tungsten impurity with 0.004% density with respect to electron density in ITER-like plasma.

(2) Helical Reactor HR-1 plasma

Figure 3 shows plasma density and temperature profile, and tungsten density radial profile of total and typical charge-states in helical ignited reactor HR-1 with typical high density low temperature operation. The tungsten impurity density becomes peaked at ρ~ 0.8 and not deeply penetrated into the plasma core, different from TR-1 case.

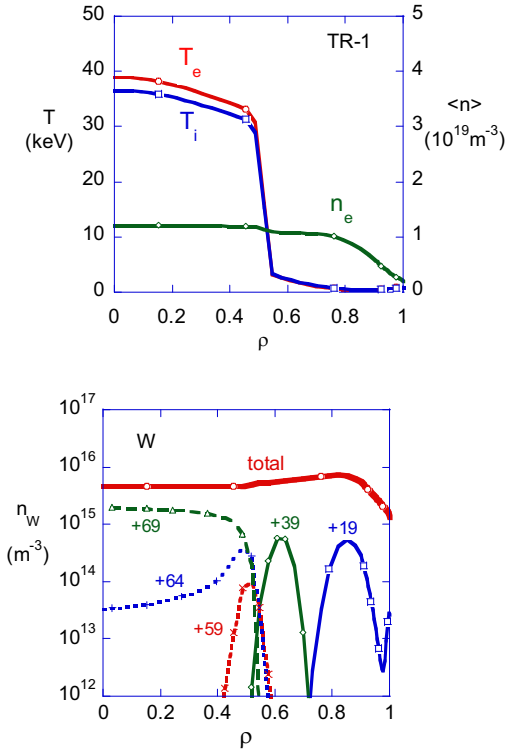

Fig. 2 Tungsten impurity profile in tokamak reactor TR-1 with ITB. (Upper) Plasma density and temperature profile. (Lower) Density profile of total and typical charge-state tungsten impurities

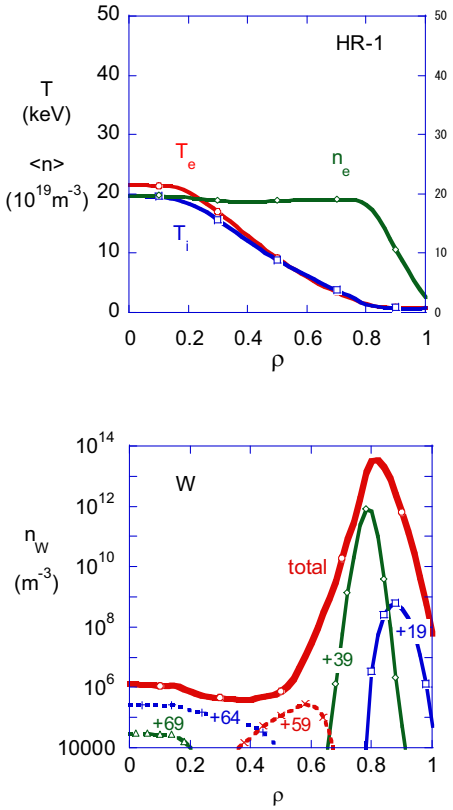

Fig.3 Tungsten impurity profile in helical reactor HR-1. (Upper) Plasma density and temperature profile. (Lower) Density profile of total and typical charge-state tungsten impurities

The operational temperature is rather low in this case and the radiation loss effects are serious to keep ignition.

4-3. Tungsten impurity control in TR-1 by edge electron density profile modification

The modification of edge plasma density might be helpful for controlling impurity influx in tokamaks. According to neoclassical theory, the normal temperature gradient (i.e. negative $\nabla T / T$) might contribute to the impurity shielding process, but normal density gradient leads to impurity pinching effect. Figure 4 shows the effect of edge electron density profile in the case of ITB at ρ=0.7~0.8. When the edge density profile becomes rather flat due to strong gradient at temperature ITB, the impurity line radiation can be reduced as shown in this figure.

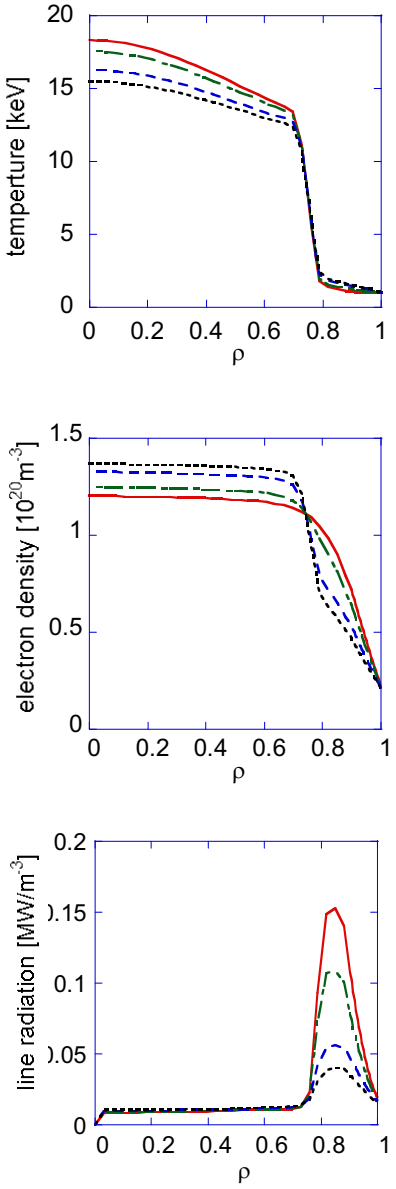

Fig. 4 Effect of modification of edge density profile on impurity transport in TR-1 tempearture-ITB plasma. Red solid and black dotted lines denote no density-ITB profile and strong density-ITB profile at ρ=0.7~0.8., respectively.

4-4. MHD effects of sawtooth and neoclassical tearing modes (NTM) on impurity dynamics

The MHD effects such as sawtooth oscillations and neoclassical tearing mode are important on the impurity behavior. The effects of these modes are already included in our TOTAL code, and the fusion power degradation due to NTM and the probability of NTM control have been evaluated using TOTAL code. These MHD effects on the impurity dynamics and its control scenarios will be described somewhere in the near future.

5. Summary and Conclusions

(1) We developed the impurity simulation code coupled with 1-D transport / 2- or 3-D equilibrium TOTAL (Toroidal Transport Analysis Linkage) code, which is applicable to tokamak and helical systems.

(2) In ITER, the critical level of impurity is, 4.0% for carbon, 0.1% for iron, and 0.008% for tungsten with respect to electron density.

(3) By the flattening of edge density profile, the impurity accumulation can be suppressed.

References

[1] K.Yamazaki, T.Amano, Nucl. Fusion **32**, 633 (1992): K. Yamazaki, Y. Higashiyama, et al, Fusion Engineering and Design **81**, 2743 (2006).

[2]Y. Murakami eta l., J.Nucl. Materials **313-316,** 1161 (2003).

[3] K.Yamazaki et al., J. Plasma Fusion Res. SERIES, **7**, 102 (2006).

[4] K.Yamazaki, T. Amano et al., Nucl. Fusion **25**, 1543 (1985).

[5] S.P.Hirshman, W.I.Van Rij, P.Merkel, Comp. Phys. Commun. **43**, 143 (1986).

[6] R. E. Waltz et al., Phys. Plasmas **4**, 2482 (1997) [7]T. Tara et al., Plasma Phys. Controlled Fusion **43**, 507(2001).

[8] W. A. Houlberg et al., Phys. Plasmas **4**, 3230(1994).

[9] T. Amano, J. Mizuno, J. Kako, 'Simulation of Impurity Transport in Tokamak, Internal report IPPJ-616, Institute of Plasma Physics, Nagoya Univ. (1982).

[10] R. A. Hulse, Nucl. Technol./Fusion **3**, 259 (1983).

[11] S. Tamor, "A Simple Fast Routine for Computation of Energy Transport by Synchrotron Radiation in Tokamaks and Similar Geometries," SAIC Report SAI-023-81-189LJ/LAPS-72 (1981).

[12] Y. Higashiyama, J.Physics: Conference Series **123**, 012032 (1008).

[13] M. H. Huges, D. E. Post, J. Comput. Phys. **28**, 43(1978).

[14] D.E Hastings, W.A. Houlberg, K.C, Shaing : Nuclear Fusion **25**, 445 (1985).

[15] K.C. Shaing and J.D. Callen, Phys. Fluids **26**, 3315 (1983).

[16] R.J.Hawryluk, S.Suckewer, and S.P.Hirshman, Nucl. Fusion **19**, 607 (1979).